NeuroImage 298 (2024) 120798

Contents lists available at ScienceDirect

NeuroImage

journal homepage: www.elsevier.com/locate/ynimg

Local functional connectivity abnormalities in mild cognitive impairment and Alzheimer's disease: A meta-analytic investigation using minimum Bayes factor activation likelihood estimation

Tommaso Costa [a,b,c,*], Enrico Premi [d], Barbara Borroni [e], Jordi Manuello [a,b], Franco Cauda [a,b,c], Sergio Duca [a,b], Donato Liloia [a,b]

[a] GCS-fMRI, Koelliker Hospital and Department of Psychology, University of Turin, Turin, Italy
[b] Functional Neuroimaging and Complex Neural Systems (FOCUS) Laboratory, Department of Psychology, University of Turin, Turin, Italy
[c] Neuroscience Institute of Turin (NIT), Turin, Italy
[d] Stroke Unit, Department of Neurological and Vision Sciences, ASST Spedali Civili, Brescia, Italy
[e] Cognitive and Behavioural Neurology, Department of Clinical and Experimental Sciences, University of Brescia, Italy

ARTICLE INFO

Keywords:
fMRI
Biomarker
NeuroSynth
Default mode network
Bayesian statistics
Bayes Factor
BrainMap
Dementia

ABSTRACT

Functional magnetic resonance imaging research employing regional homogeneity (ReHo) analysis has uncovered aberrant local brain connectivity in individuals with mild cognitive impairment (MCI) and Alzheimer's disease (AD) in comparison with healthy controls. However, the precise localization, extent, and possible overlap of these aberrations are still not fully understood. To bridge this gap, we applied a novel meta-analytic and Bayesian method (minimum Bayes Factor Activation Likelihood Estimation, mBF-ALE) for a systematic exploration of local functional connectivity alterations in MCI and AD brains. We extracted ReHo data via a standardized MEDLINE database search, which included 35 peer-reviewed experiments, 1,256 individuals with AD or MCI, 1,118 healthy controls, and 205 x-y-z coordinates of ReHo variation. We then separated the data into two distinct datasets: one for MCI and the other for AD. Two mBF-ALE analyses were conducted, thresholded at "very strong evidence" (mBF $\geq$ 150), with a minimum cluster size of 200 mm^3. We also assessed the spatial consistency and sensitivity of our Bayesian results using the canonical version of the ALE algorithm. For MCI, we observed two clusters of ReHo decrease and one of ReHo increase. Decreased local connectivity was notable in the left precuneus (Brodmann area – BA 7) and left inferior temporal gyrus (BA 20), while increased connectivity was evident in the right parahippocampal gyrus (BA 36). The canonical ALE confirmed these locations, except for the inferior temporal gyrus. In AD, one cluster each of ReHo decrease and increase were found, with decreased connectivity in the right posterior cingulate cortex (BA 30 extending to BA 23) and increased connectivity in the left posterior cingulate cortex (BA 31). These locations were confirmed by the canonical ALE. The identification of these distinct functional connectivity patterns sheds new light on the complex pathophysiology of MCI and AD, offering promising directions for future neuroimaging-based interventions. Additionally, the use of a Bayesian framework for statistical thresholding enhances the robustness of neuroimaging meta-analyses, broadening its applicability to small datasets.

1. Introduction

Mild cognitive impairment (MCI) can be considered as an intermediate state between normal aging and Alzheimer's Disease (AD) and it is mostly characterized by memory deficits, but with normal activities of daily living (Klekociuk et al., 2016). Considering the growing field of potential disease-modifying treatments, it is mandatory to elucidate the neurobiology of MCI, to obtain the greatest likelihood to modify the natural history of the disease with pharmacological (or non-pharmacological) interventions (Márquez and Yassa, 2019). Over the past 30 years, significant advancements in technology related to functional magnetic resonance imaging (fMRI) have provided an unparalleled environment for in-vivo assessment of the neurobiological substrate of dementias. Notably, resting-state fMRI (rs-fMRI), a

* Corresponding author at: Department of Psychology, Via Verdi 10, 10124 Turin, Italy.
E-mail address: tommaso.costa@unito.it (T. Costa).

https://doi.org/10.1016/j.neuroimage.2024.120798
Received 24 April 2024; Received in revised form 13 August 2024; Accepted 15 August 2024
Available online 15 August 2024

well-established set of methods capable of detecting spontaneous low-frequency regional temporal correlations in the Blood Oxygen Level-Dependent (BOLD) signal, has emerged as a valuable tool for investigating the disrupted brain functional connectivity of the pathological human brain. Previous rs-fMRI research has predominantly concentrated on abnormalities in long-range connectivity using predetermined regions-of-interest, revealing patterns of hypo-connectivity in distinct cohorts of individuals with MCI and AD (Badhwar et al., 2017; Brier et al., 2014; Ibrahim et al., 2021). By contrast, the establishment of local (or short-range) functional connectivity abnormalities remains less robust, primarily due to the absence of sound fMRI-based metrics. Nevertheless, exploring local functional connectivity aberrations for neurodegenerative conditions holds promise for providing a precise definition of candidate diagnostic and prognostic biomarkers at the brain level (Liu et al., 2021; Wang et al., 2021).

Independent research endeavors have been dedicated to unveiling atypical local functional connectivity in MCI through the application of regional homogeneity (ReHo). ReHo, a voxel-wise rs-fMRI technique, utilizes Kendall's coefficient of concordance to examine the coherence of time series of the BOLD signal amplitude within small clusters of neighboring voxels (Jiang and Zuo, 2016; Zang et al., 2004). The data-driven whole-brain nature of the method and its demonstrated high test–retest reliability (Zuo et al., 2013) have contributed valuable insights into the spatial distribution of aberrant local connectivity in MCI, appearing to be concentrated in diverse brain regions associated with visual, default mode, attentional, and sensorimotor networks (Cha et al., 2015; Min et al., 2019; Yuan et al., 2016; Yue et al., 2023). Notwithstanding the significance of these findings, it is imperative to recognize the inherent inconsistency observed in the outcomes of research efforts. Recent neuroimaging meta-analyses (C. Yang et al., 2023; X. Yang et al., 2023; Zhen et al., 2018) have successfully identified consistent changes in ReHo among individuals with MCI in comparison to healthy controls (HCs), encompassing prefrontal, temporo-parietal, limbic, and cerebellar regions. However, the specific localization of these changes varies markedly across different studies (refer to **Fig. S1** for the neuroanatomical distribution of observed ReHo variations in previous meta-analyses conducted on MCI).

Somewhat unexpectedly, the exploration of ReHo in AD has been relatively limited to date. Part of this body of research has revealed concurrent patterns of both local hypo- and hyper-connectivity, spanning neocortical, limbic, and cerebellar territories (He et al., 2007; Peraza et al., 2016). Other discrepancies emerge in this literature, as certain studies singularly point to either decreased or increased ReHo aberrations in AD when compared to HCs (Liao et al., 2022; Marchitelli et al., 2018). Finally, conflicting effects have been observed in hub nodes of the human connectome, such as the cingulate cortex, precuneus, and superior temporal cortex (Cha et al., 2015; He et al., 2007; Peraza et al., 2016). Hence, there exists a compelling interest in addressing the prevailing inconsistency and systematically characterizing ReHo alterations in individuals with AD by quantitatively aggregating the existing studies. To date, no comprehensive study has undertaken this endeavor. This gap in the literature underscores a critical need, as such an investigation holds potential significance for the advancement of neuroimaging-based interventions. Additionally, it may contribute to delineating the specific or shared local functional alterations occurring in MCI and AD, a matter of particular importance given the scarcity of direct comparisons and the inherent inconsistencies in the available findings (Zhang et al., 2021, 2012).

Within the context delineated, the primary objective of this study is to conduct a comprehensive meta-analysis using the most extensive compilation of ReHo studies in MCI and AD available to date. This investigation is designed to achieve two principal goals: firstly, to elucidate consistent changes in local brain connectivity in MCI and AD when compared to HCs; and secondly, to discern functional distinctions and commonalities between the conditions, shedding light on potential shared and/or distinct neuropathological pathways throughout the AD continuum. To this end, we employed the minimum Bayes Factor version of the activation likelihood estimation (ALE) algorithm (Costa et al., 2023), a recently developed Bayesian implementation of the most widely utilized neuroimaging meta-analytic method globally. This updated statistical threshold not only assesses the spatial convergence of functional variations among the outcomes of previously published studies, but also offers several advantages over traditional thresholding ALE procedures. Distinctive features include its capacity to provide informative insights into the probabilities associated with the validity of considered hypotheses, unlike conventional approaches that solely offer a rejection criterion for the null hypothesis based on a critical p-value (Liloia et al., 2023). Still, it eliminates the prerequisite for a minimum number of studies in the ALE environment to generate unbiased results, enhancing the robustness of the findings (Costa et al., 2021; Eickhoff et al., 2016). To enhance the elucidation of the neurophysiological foundation underlying ReHo aberrations in MCI and AD, we also conducted an examination of large-scale network functional connectivity and cognitive processes statistically associated with the observed ReHo clusters of variation. This analysis was facilitated through the utilization of the Neurosynth database (Yarkoni et al., 2011), providing an interpretation of our findings from an observer-independent and unbiased perspective.

2. Materials and methods

2.1. Search strategy and data selection

The study design adhered to established guidelines for neuroimaging meta-analyses (Manuello et al., 2022; Müller et al., 2018) and followed PRISMA statement quality criteria (Page et al., 2021). A systematic literature search was conducted in the PubMed database using these two sets of keywords: (search a) "*mild cognitive impairment*" OR "*MCI*" OR "*aMCI*" AND "*regional homogeneity*" OR "*ReHo*" OR "*local connectivity*"; (search b) "*Alzheimer's disease*" OR "*AD*" AND "*regional homogeneity*" OR "*ReHo*" OR "*local connectivity*". Furthermore, reference lists of pertinent reviews and meta-analyses (Badhwar et al., 2017; X. Yang et al., 2023; C. Yang et al., 2023; Zhen et al., 2018) were scrutinized to identify eligible articles. The search was updated until December 2023, without imposing restrictions on publication years.

Screening identified records based on the following inclusion criteria: (i) original peer-reviewed English-language journal articles; (ii) experiments investigating ReHo voxel-wise differences between subjects with MCI or AD and HCs at the whole-brain level; (3) experiments reporting significant results and coordinates (x–y-z foci) of clusters of ReHo changes using a stereotactic space. Records exclusion was based on: (i) case report, conference abstract, or review articles; (ii) animal model investigations; (iii) absence of between-group comparison with HCs; (iv) sample sizes < 7 participants per group; (v) experiments focused on specific brain regions (i.e., region-of-interest and/or small volume correction analyses); (vi) analysis of no resting-state fMRI data (i.e., ReHo data derived from task-based fMRI experiments). Ultimately, to mitigate the risk of spurious results stemming from population overlap, multiple ReHo experiments within a single article were taken into account only when reporting on independent clinical groups (Liloia et al., 2024a).

The articles were first extracted by two authors (LD and CT). The full-texts of the relevant articles were then independently evaluated by three authors (LD, CT, and EP). Disagreements were resolved by unanimous consensus. Peak coordinates of abnormal ReHo clusters were extracted from all included ReHo experiments. Our analyses were carried out in MNI space. To enhance the spatial accuracy of the meta-analysis, we employed the icbm2tal algorithm (Laird et al., 2010). This algorithm facilitated the conversion of experimental result coordinates initially reported in Talairach space to the MNI space.

2.2. Data analysis

To ascertain the presence of consistent patterns of ReHo variation in individuals with MCI and AD, as well as to determine the force of evidence of our findings, we used both Bayesian-based and canonical versions of the activation likelihood estimation (ALE) method.

Specifically, we firstly adopted the recent version of the ALE algorithm using a minimum Bayes Factor (mBF) thresholding (Costa et al., 2023) as implemented in the MATLAB® script available at https://figshare.com/articles/software/minimum_bayes_factor_script/17023931. Following the distribution of the evidence categories for the Bayes Factor proposed by Kass and Raftery (Kass and Raftery, 1995), the mBF-ALE threshold was set at strong evidence (i.e., BF $\geq$ 20) and very strong evidence (i.e., BF $\geq$ 150), with a cluster size $\geq$ 200 mm^3. Thus, we also evaluated the spatial consistency and sensitivity of our primary findings using the canonical version of the ALE algorithm implemented in the GingerALE software package (v.3.0.2; https://brainmap.org/software.html#GingerALE) (Eickhoff et al., 2012) re-analyzing the same data set. Following the recently recommended ALE setting (Eickhoff et al., 2016), ALE results were family-wise error-corrected (FWE-c) for multiple comparisons, with a cluster-level inference of $p <$ .05, a cluster-forming threshold of $p <$ .001 on the voxel-level (1000 permutation runs), and a with a cluster size $\geq$ 200 mm^3.

2.2.1. Anatomical likelihood estimation (canonical version)

The ALE technique furnishes insights into the spatial convergence of coordinates across the selected neuroimaging literature. In this context, each reported coordinate in a neuroimaging experiment is regarded as the center of a Gaussian probability distribution, defined as:

$$p(d) = \frac{1}{\sigma^2 \sqrt{(2\pi)^3}} e^{-\frac{d^2}{2\sigma^2}}$$

Here, d represents the Euclidean distance between the coordinate and the surrounding voxels, while σ signifies the spatial uncertainty. For each selected experiment, a modeled alteration (MA) map is computed, representing the union of all Gaussian distributions associated with that experiment. The integration of all MA maps produced the final ALE map. The significance of each voxel was assessed against a null-hypothesis derived from an iterative random distribution of the coordinates. The cluster-level threshold was hence established through a Monte Carlo simulation of a cluster size distribution. For detailed technical information about the method, consult Eickhoff et al. (2009).

2.2.2. Activation likelihood estimation (minimum Bayes factor version)

The mBF-ALE technique offers insights into the spatial convergence of coordinates across the chosen neuroimaging literature. Importantly, it possesses the capability to furnish informative perspectives on the probabilities associated with the validity of considered hypotheses, even in the context of small meta-analytic datasets. The computation of the mBF relies on Bayes' theorem. In accordance with this theorem, the probability linked to two simultaneous hypotheses, denoted as H_0 and H_1, can be formally expressed as follows:

$$P(H_0|D) = \frac{P(D|H_0)}{P(D)} P(H_0)$$

and, correspondingly

$$P(H_1|D) = \frac{P(D|H_1)}{P(D)} P(H_1)$$

where D is the measured effect for each brain voxel. Their quotient represents the Bayes' theorem in terms of relative belief:

$$\frac{P(H_0|D)}{P(H_1|D)} = \frac{P(D|H_0)}{P(D|H_1)} \frac{P(H_0)}{P(H_1)}$$

Derived from the preceding formulas, the expression for BF_{01} can be articulated as follows:

$$BF_{01} = \frac{P(D|H_0)}{P(D|H_1)}$$

The BF_{01} value quantifies the strength of evidence for two concurrent hypotheses: a $BF_{01} > 1$ supports the evidence favoring H_0, while a $BF_{01} < 1$ supports H_1. Traditionally, using the Bayes Factor to gauge evidence for a composite hypothesis involves averaging all potential distinct alternative values. However, in scenarios where infinite alternative values exist, such as the hypothesis "the mean is different from zero", a method is required to address this. To overcome this challenge, the approach involves selecting the alternative value with the most substantial effect against the null hypothesis. This value is considered a summary of evidence across all possible distinct values within the composite alternative hypothesis and is termed the minimum Bayes Factor (mBF). The mBF, therefore, represents the most compelling evidence against the null hypothesis.

Now, consider the hypothesis as the probability of a generic observed effect x modeled through a Gaussian distribution with mean μ and variance σ^2 :

$$p(x|\mu, \sigma) = \frac{1}{\sigma\sqrt{2\pi}} e^{-\frac{(x-\mu)^2}{2\sigma^2}}$$

the BF for the null-hypothesis versus the supported hypothesis ($\mu = x$) is the mBF:

$$mBF_{01} = e^{-\frac{x^2}{2\sigma^2}}$$

Upon utilizing the Z map derived from the unthresholded ALE map, the computation of the mBF can be achieved by applying the following formula:

$$mBF_{01} = e^{-\frac{Z^2}{2}}$$

by applying a simple exponentiation. This signifies the strength of evidence supporting the null-hypothesis H_0 over the alternative hypothesis H_1.

The mBF varies across a range from 0 to ∞. As per Kass and Raftery (Kass and Raftery, 1995), the interpretation of values can be delineated as illustrated in Table 1.

2.2.3. Amnestic mild cognitive impairment sub-analysis

A subgroup meta-analytic investigation was undertaken to elucidate consistent patterns of ReHo variation specifically observed in ReHo experiments analyzing individuals with MCI who have an explicitly reported amnestic phenotype (i.e., amnestic mild cognitive impairment; aMCI). This analysis is particularly pertinent as aMCI is characterized by prominent memory impairment and is associated with a heightened risk of progression to AD neuropathology compared to non-amnestic MCI presentations (Dubois and Albert, 2004; Forlenza et al., 2009; Petersen et al., 2014).

2.2.4. Meta-regression analysis

We employed the seed-based d mapping software (v.6.21) (Albajes-Eizagirre et al., 2019) to perform a series of voxel-wise meta-regression

Table 1
The evidence categories for the Bayes Factor (BF). Adapted from Kass & Raftery.

BF_{10} value	Force of evidence
1 - 3	Very weak
3 - 20	Positive
20 - 150	Strong
> 150	Very strong

analyses. These post-hoc analyses aimed to investigate the potential influence of socio-demographic, clinical, and methodological variables on both MCI and AD meta-analytic ReHo findings. Specifically, we assessed the impacts of mean age at the scan session, sex distribution (i.e., percentage of males), mean years of education, sample size, and cognitive impairment (i.e., mean score of the mini-mental state examination test). Details of the data included in these analyses are summarized in Table 2. We also evaluated the effects of MRI field strength and image smoothing level. Details of the data included in these analyses are summarized in **Table S1**. ReHo experiments missing these measures were excluded from the analysis. To achieve an optimal balance between specificity and sensitivity (Radua et al., 2012), we adopted a voxel-level threshold of $p < .0005$ and a minimum cluster size of 150 mm^3.

2.2.5. Contrast data analysis

A comprehensive whole-brain voxel-wise comparison analysis was performed to identify shared regions exhibiting ReHo variations between MCI and AD. This involved the comparison of canonical ALE maps, as well as mBF-ALE maps for MCI and AD, with thresholds set at strong evidence (BF $\geq$ 20) and very strong evidence (BF $\geq$ 150), along with a minimum cluster size of $\geq$ 10 mm^3.

2.2.6. Cognitive association analysis

The NeuroSynth meta-analytic tool was used to estimate the association between regions with significant ReHo variations and relevant cognitive terms. By utilizing high-frequency keywords associated with functional MRI stereotactic coordinates, NeuroSynth taps into findings from over 15,000 published fMRI studies (https://github.com/neurosynth). This estimation is grounded in the likelihood of a given cognitive function being mentioned alongside the activation of a specific region-of-interest (ROI). In our study, ROIs were defined as 10-mm radius areas surrounding the local peak of each altered ReHo cluster. The values used are derived from quantitative estimates of spatial uncertainty associated with stereotactic coordinates in the ALE environment, indicating a mean spatial uncertainty of 10.2 mm (StDev = 0.4 mm) (Eickhoff et al., 2009; Liloia et al., 2021). The estimate from NeuroSynth offers a quantitative measure of the relationship between abnormal brain areas and cognitive processes. Following prior studies (Hansen et al., 2021; Liloia et al., 2024b, 2024a), we exclusively focused on concepts from the Cognitive Atlas (Poldrack et al., 2011) (i.e., 886 concepts at the time of analysis).

2.2.7. Large-scale functional networks decomposition

To quantitatively delineate the functional localization of identified ReHo variations in MCI and AD, we delved into their impact on large-scale functional networks. Specifically, we examined the distribution of ReHo variation voxels from mBF-ALE analyses across different brain networks. We adopted the network parcellation introduced by Yeo et al. (Yeo et al., 2011), which delineates the human brain cortex into seven functionally distinct networks based on resting-state fMRI data from 1000 healthy human subjects.

3. Results

The literature searches identified 1374 articles. After the title/abstract screening, 124 records were evaluated at the full-text level. A total of 35 ReHo experiments coming from 27 different articles were included in the quantitative synthesis. PRISMA flow charts are reported in **Fig. S2**. In detail, the MCI group included 28 ReHo experiments, for a total of 1010 subjects compared with 954 HCs and 143 coordinates of alteration (78 of ReHo decrease and 65 of ReHo increase; Fig. 1**A**). The aMCI sub-group included 16 ReHo experiments, for a total of 600 subjects compared with 622 HCs and 99 coordinates of alteration (59 of ReHo decrease and 40 of ReHo increase). The AD group included seven ReHo experiments, for a total of 246 subjects compared with 229 HCs and 62 coordinates of alteration (50 of ReHo decrease and 12 of ReHo increase; Fig. 2**A**). Detailed clinical and methodological information about the MCI and AD groups are summarized in Table 2 and **Table S1**.

3.1. Local connectivity changes in mild cognitive impairment

mBF-ALE (thresholded at strong evidence). Compared to HCs, subjects with MCI showed seven clusters of ReHo decrease and 14 clusters of ReHo increase, respectively (**Fig. S3A** and **Table S2**). Local peaks of decreased local connectivity were found in the left precuneus (Brodmann area – BA 7), right supramarginal gyrus (BA 40), left inferior temporal gyrus (ITG; BA 20), right globus pallidus, right posterior cingulate cortex (PCC; BA 30), right middle frontal gyrus (BA 46), and left precentral gyrus (BA 6). By contrast, increased local connectivity was found in the right parahippocampal gyrus (BA 36), left lingual gyrus (BA 18), left inferior parietal lobule (BA 39), right postcentral gyrus (BA 40), left cuneus (BA 17), left inferior frontal gyrus (IFG; BAs 9 and 44), right paracentral lobule (BA 5), right culmen of the cerebellum, bilateral putamen, left caudate body, right anterior cingulate cortex (ACC; BA 24), and left precuneus (BA 7). Sub-analysis of the aMCI phenotype revealed statistically significant clusters that largely overlapped with those identified in the main MCI analysis (**Table S2**).

mBF-ALE (thresholded at very strong evidence). Compared to HCs, subjects with MCI showed two clusters of ReHo decrease and one cluster of ReHo increase, respectively (Fig. 1**B** and Table 3). Local peaks of decreased local connectivity were found in the left precuneus (BA 7) and left ITG (BA 20). By contrast, increased local connectivity was found in the right parahippocampal gyrus (BA 36). The analysis of the aMCI sub-group revealed statistically significant clusters that overlapped with those identified in the primary MCI analysis, except for the cluster located in the left BA 20 (Table 3).

Canonical ALE (thresholded at cluster-level). Compared to HCs, subjects with MCI showed one cluster of ReHo decrease and one cluster of ReHo increase, respectively (Fig. 1**C** and Table 3). Local peak of decreased local connectivity was found in the left precuneus (BA 7). By contrast, increased local connectivity was found in the right parahippocampal gyrus (BA 36). The analysis of aMCI sub-group revealed statistically significant clusters that overlapped with those identified in the primary MCI analysis.

3.2. Local connectivity changes in Alzheimer's disease

mBF-ALE (thresholded at strong evidence). Compared to HCs, subjects with AD showed 17 clusters of ReHo decrease and 10 clusters of ReHo increase, respectively (**Fig. S3B** and **Table S3**). Local peaks of decreased local connectivity were found in the bilateral PCC (BAs 23, 30, and 31), left medial frontal gyrus (BA 10), left superior parietal lobule (BA 40), left precuneus (BA 7), left cuneus (BA 17), right middle occipital gyrus (BA 18), right precentral gyrus (BA 4), left ACC (BA 24), left superior temporal gyrus (BAs 22), left postcentral gyrus (BA 2), bilateral middle temporal (BA 39) and left supramarginal gyrus (BA 40). By contrast, increased local connectivity was found in the left ITG (BA 19), right declive of the cerebellum, left PCC (BA 31), left precuneus (BA 7), left IFG (BA 44), and in the bilateral cuneus (BA 18) and lingual gyrus (BA 19).

mBF-ALE (thresholded at very strong evidence). Compared to HCs, subjects with AD showed one cluster of ReHo decrease and one cluster of ReHo increase, respectively (Fig. 2**B** and Table 4). The peak of decreased local connectivity was found in the right PCC (BA 30 extending to BA 23). By contrast, increased local connectivity was found in the left PCC (BA 31).

Canonical ALE (thresholded at cluster-level). Compared to HCs, subjects with AD showed one cluster of ReHo decrease and one cluster of ReHo increase, respectively (Fig. 2**B** and Table 4). The peak of decreased local connectivity was found in the right PCC (BA 30 extending to BA 23). Increased local connectivity was found in the left PCC (BA 31).

Table 2
Regional homogeneity experiments included in the activation likelihood estimation meta-analyses of mild cognitive impairment (A) and Alzheimer's disease (B): demographic and clinical details.

No.	Author (sub-group)	Year	Diagnosis	Sample (%male)		Age (SD)		Education (SD)		MMSE (SD)		ReHo	changes
				Patients	Controls	Patients	Controls	Patients	Controls	Patients	Controls	Pat < HC	Pat > HC
(A) Mild Cognitive Impairment													
1	Bai et al. (1)	2008	aMCI	20(50)	20(45)	71.3(3.8)	69.4 (3.8)	14(3.1)	13.8(4)	27.2 (1.6)	28.3 (1.4)	9	4
2	Zhang et al. (2)	2012	aMCI	19(52.6)	21(63.1)	76(8)	70(7)	N/A	N/A	27(2)	29(1)	0	6
3	Liu Z et al. (3)	2014	aMCI	12(8.3)	12(33.3)	59.3(3.3)	60.6 (5.8)	10.5 (1.8)	10.6 (2.1)	26.4 (0.9)	29.9 (0.4)	4	4
4	Cha et al. (4)	2015	aMCI	34(52.9)	62(27.4)	68.4(7.9)	68.5(8)	11.5 (5.2)	10.9 (5.2)	27.1 (2.1)	28.6 (1.9)	13	0
5	Wang et al. (5)	2015	MCI	30(60)	32(46.9)	69.1(5.8)	70.1 (5.5)	N/A	N/A	26.2 (2.2)	28.1 (1.5)	5	6
6	Ni et al. (6)	2016	MCI	26(46.2)	28(60.7)	71(9)	70(9)	12(3.1)	15(1.4)	25(1.5)	29(1.1)	1	5
7	Long et al. (7)	2016	MCI	29(44.8)	32(37.5)	66.5(8.4)	62.9 (8.1)	10.1 (4.5)	11(4.1)	23.4(3)	27.9 (1.6)	1	2
8	Yuan et al. (8)	2016	aMCI	36(47.2)	46(41.3)	66.8(9.5)	64.3 (7.8)	10(4.1)	11.4 (5.1)	24.9 (3.4)	28.5(2)	8	7
9	Cai et al. (R group) (9)	2018	MCI	20(55)	53(54.7)	69.8(6.5)	76.1 (6.5)	N/A	N/A	25.6 (2.7)	28.2 (2.1)	1	1
10	Cai et al. (S group) (9)	2018	MCI	50(52)	53(54.7)	72.3(6.9)	76.1 (6.5)	N/A	N/A	24.3 (2.5)	28.2 (2.1)	1	1
11	Cai et al. (P group) (9)	2018	MCI	32(47)	53(54.7)	74(6.1)	76.1 (6.5)	N/A	N/A	22.9 (2.1)	28.2 (2.1)	2	2
12	Kang et al. (10)	2018	aMCI	34(20.6)	38(50)	76.1(4.7)	74(5.4)	9.4(4.7)	11.7(5)	22.7 (3.9)	26.3 (2.3)	3	5
13	Luo et al. (SD group) (11)	2018	aMCI	32(53.1)	49(36.7)	72.4(4.3)	73.3 (4.6)	16.5 (2.6)	16.2 (2.6)	28.3 (1.7)	29(1.2)	1	2
14	Luo et al. (MD group) (11)	2018	aMCI	32(53)	49(36.7)	74.9(5.3)	73.3 (4.6)	15.3 (2.7)	16.2 (2.6)	27.2 (1.7)	29(1.2)	1	0
15	Min et al. (12)	2019	aMCI	10(50)	10(50)	69.8(2.7)	69.9 (2.6)	13.2 (1.1)	13.6 (1.7)	25.9 (0.7)	29.3 (0.8)	5	4
16	Zuo et al. (13)	2019	MCI	31(58)	32(56.2)	63.8 (14.1)	62.7 (8.2)	9.3(2.1)	10.2 (2.3)	26.3 (2.1)	28.7 (1.4)	2	0
17	Zhang et al. (14)	2020	aMCI	98(60.2)	64(42.2)	73.7(6.8)	75.6(6)	16.8 (2.6)	16.4 (2.5)	28.4 (1.6)	29(1.4)	1	0
18	Liu et al. (15)	2021	MCI	28(50)	38(47.4)	68.4(4.7)	68.7 (5.1)	9(2.8)	10.4 (3.5)	N/A	N/A	2	0
19	Zhang Q et al. (16)	2021	aMCI	20(40)	20(60)	71.9(5.9)	70.7 (5.4)	11.4 (3.7)	13.4 (2.9)	26.9 (2.1)	28.6 (1.2)	2	0
20	Zhang Z. et al. (17)	2022	aMCI	28(46.4)	37(40.5)	65.7(6.9)	63.9 (8.4)	12.2 (3.2)	12.2 (3.4)	27(N/A)	29(N/A)	3	1
21	Hu et al. (18)	2022	MCI	32(59.4)	37(62.2)	75.4(7.9)	73.4(7)	16.7 (2.5)	16.9 (2.4)	28.9 (1.4)	29.1(1)	0	2
22	Liu et al. (19)	2022	aMCI	114 (40.4)	101 (35.6)	72.4(5.2)	71.7(5)	10.8 (2.6)	10.2 (2.7)	24.1(1)	28.3(1)	4	0
23	Wu et al. (20)	2022	MCI	12(50)	12(50)	64.3(7)	64(6.2)	N/A	N/A	21.4 (4.6)	27.8 (2.5)	2	5
24	Gao et al. (21)	2022	MCI	53(N/A)	68(50)	69.1(4.9)	68.8 (4.9)	10(3.3)	9.7(3.4)	N/A	N/A	1	0
25	Wu et al. (22)	2023	aMCI	40(45)	42(38)	64.5(8)	63.8 (7.3)	11.9 (3.1)	11.8 (3.3)	27.5(N/A)	29(N/A)	1	0
26	Yue et al. (23)	2023	aMCI	26(53.8)	26(53.8)	62(2.7)	60.6 (3.9)	13.1(2)	13.5 (1.9)	25.6 (1.2)	29.8 (0.4)	2	7
27	Zhong et al. (NA group) (24)	2023	MCI	64(34.4)	74(27.7)	67.6(7.7)	66.1(5)	9(3.6)	10.8 (2.9)	25.4 (2.4)	27.2(2)	1	1
28	Zhong et al. (A group) (24)	2023	aMCI	45(30)	74(27.7)	66.8(8.3)	66.1(5)	8.4(3.6)	10.8 (2.9)	24.6 (2.9)	27.2(2)	2	0
(B) Alzheimer's Disease													
1	He et al. (25)	2007	AD	14(42.8)	14(42.8)	70.1(6.4)	69.6 (5.5)	9.4(4.9)	9.4(4.2)	23.2 (2.8)	28.8(1)	1	4
2	Zhang et al. (2)	2012	AD	23(30.4)	21(63.1)	73(9)	70(7)	N/A	N/A	20(4)	29(1)	24	0
3	Cha et al. (4)	2015	AD	37(27)	62(27.4)	72.8(8.2)	68.5(8)	10.9 (5.3)	10.9 (5.2)	16.8 (6.9)	28.6 (1.9)	16	0
4	Peraza et al. (26)	2016	AD	18(83.3)	16(72.2)	75.4(8.6)	76.7 (5.9)	N/A	N/A	21.8 (3.8)	29.1 (0.9)	1	7
5	Marchitelli et al. (27)	2018	AD	17(58.8)	23(30.4)	72(6)	64(13)	N/A	N/A	21(3.8)	29(2)	3	0
6	Zhang Q et al. (16)	2021	AD	20(50)	20(60)	73(6)	70.7 (5.4)	10.7 (3.5)	13.4 (2.9)	19.6 (3.3)	28.6 (1.2)	5	0
7	Liao et al. (28)	2022	AD	111 (33.3)	73(43.8)	68.3(9.6)	66.3 (9.5)	7.9(4.4)	8.3(3.4)	17.2 (5.6)	28.8 (0.8)	0	1

AD, Alzheimer's Disease; aMCI, amnestic mild cognitive impairment; HC, healthy control group; MCI, mild cognitive impairment; N/A, data not associated; PAT, patients; SD, standard deviation.

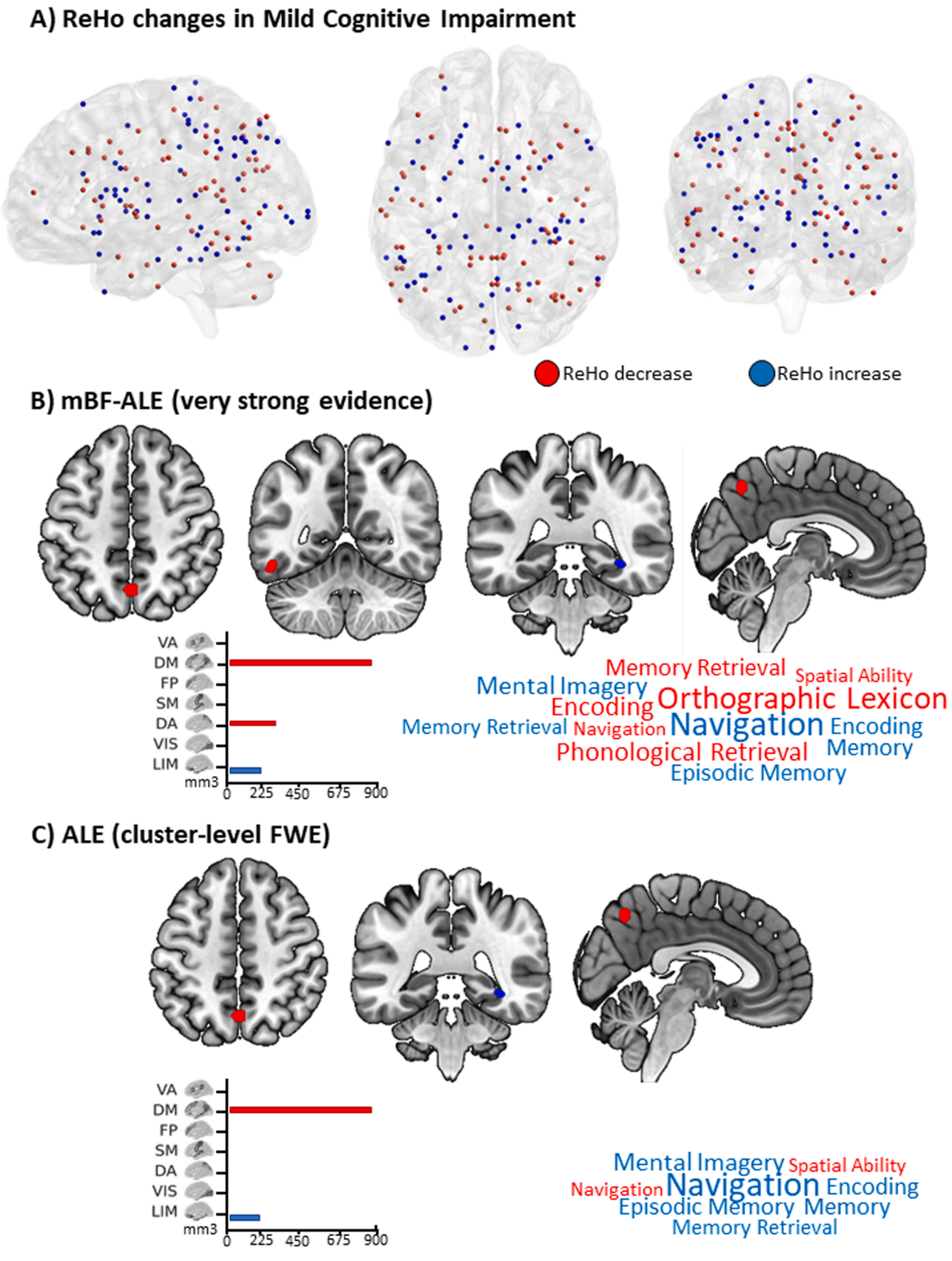

(caption on next page)

Fig. 1. Results of mild cognitive impairment (MCI) meta-analysis. (A) Neuroanatomical distribution of regional homogeneity variation findings selected from included experiments. Brain clusters of regional homogeneity decrease (red) and increase (blue) in subjects with mild cognitive impairment compared to healthy controls using the minimum Bayes Factor version of the activation likelihood estimation thresholded at very strong evidence (A) and using the cluster-level family-wise error rate (FWE) version of the activation likelihood estimation (B). Findings are visualized as coronal/axial/sagittal slices (2-D cortical, subcortical, and cerebellar view) in neurological convention. Below, the functional network decomposition results (bar charts represent the number of mm^3 of regional homogeneity variation in subjects with mild cognitive impairment compared to healthy controls) and the cognitive processes statistically related to the ALE findings according to the Neurosynth database (font sizes represent the magnitude of the associated Z-scores). ALE = activation likelihood estimation; mBF = minimum Bayes Factor; VA = ventral Attention network; DM = default mode network; FP = frontoparietal network; SM = somatomotor network; DA = dorsal attention network; VIS = visual network; LIM = limbic network.

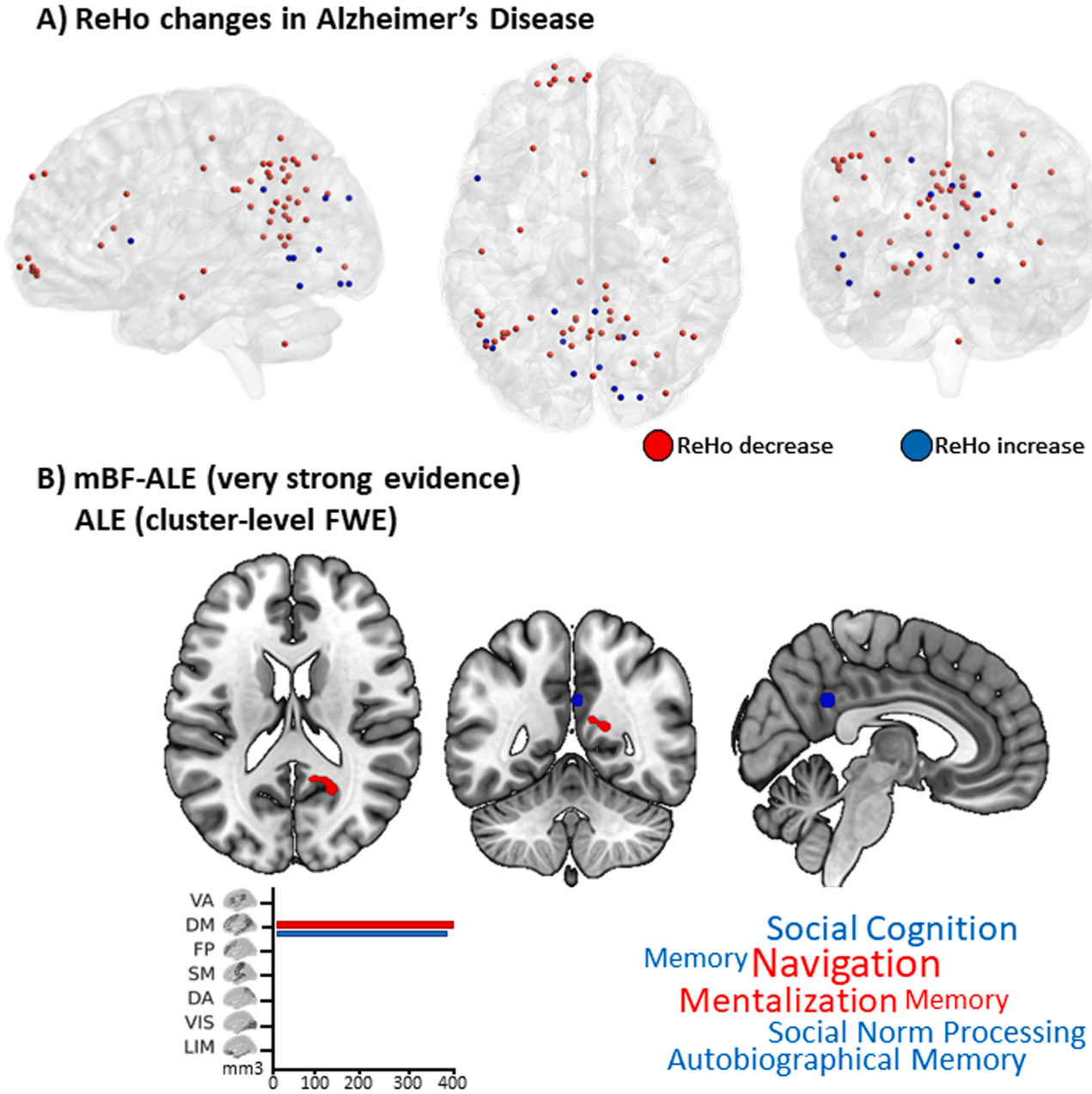

Fig. 2. Results of Alzheimer's disease (AD) meta-analysis. (A) Neuroanatomical distribution of regional homogeneity variation findings selected from included experiments. (B) Brain clusters of regional homogeneity decrease (red) and increase (blue) in subjects with Alzheimer's disease compared to healthy controls using both the minimum Bayes Factor version of the activation likelihood estimation thresholded at very strong evidence and using the cluster-level family-wise error rate (FWE) version of the activation likelihood estimation. Findings are visualized as coronal/axial/sagittal slices (2-D cortical, subcortical, and cerebellar view) in neurological convention. Below, the functional network decomposition results (bar charts represent the number of mm^3 of regional homogeneity variation in subjects with Alzheimer's compared to healthy controls) and the cognitive processes statistically related to the ALE findings according to the Neurosynth database (font sizes represent the magnitude of the associated Z-scores). ALE = activation likelihood estimation; mBF = minimum Bayes Factor; VA = ventral Attention network; DM = default mode network; FP = frontoparietal network; SM = somatomotor network; DA = dorsal attention network; VIS = visual network; LIM = limbic network.

Table 3
Clusters of regional homogeneity variation in mild cognitive impairment compared with healthy controls.

Cluster	Brain Region (Local Maxima)	MNI			Cluster Size (mm^3)	mBF Value (Very Strong Evidence)		Frequentist ALE (Cluster-level)
		x	y	z		Maximum	Minimum	
MCI < HCs								
1	Left Precuneus (BA 7)*,§	0	−62	50	874	1,388,879	150	Yes
2	Left ITG (BA 20)	−52	−54	−14	276	1525	150	No
MCI > HCs								
1	Right Parahippocampus (BA 36)*,§	36	−38	−8	208	2023	150	Yes

BA = Brodmann area; ITG = inferior temporal gyrus; MNI = Montreal Neurological Institute; mBF = minimum Bayes Factor; ALE = activation likelihood estimation.
* = brain cluster also identified via canonical ALE algorithm with a cluster-level inference of $p < .05$, and a cluster-forming threshold of $p < .001$ on the voxel-level.
§ = brain cluster also identified for the amnestic mild cognitive impairment (aMCI) sub-group using the mBF-ALE algorithm and thresholded at very strong evidence.

Table 4
Clusters of regional homogeneity variation in Alzheimer's disease compared with healthy controls.

Cluster	Brain Region (Local Maxima)	MNI			Cluster Size (mm^3)	mBF Value (Very Strong Evidence)		Frequentist ALE (Cluster-level)
		x	y	z		Maximum	Minimum	
AD < HCs								
1	Right PCC (BA 30)*	22	−58	18	400	2153	150	Yes
AD > HCs								
1	Right PCC (BA 31)*	2	−48	30	383	8246	150	Yes

BA = Brodmann area; PCC = posterior cingulate cortex; MNI = Montreal Neurological Institute; mBF = minimum Bayes Factor; ALE = activation likelihood estimation.
* = brain cluster also identified via canonical ALE algorithm with a cluster-level inference of $p < .05$, and a cluster-forming threshold of $p < .001$ on the voxel-level.

3.3. Effects of clinical, socio-demographic, and methodological variables

Several moderators were examined to understand their between-experiment influence on published ReHo findings in MCI and AD. No significant linear associations were found with age, sex distribution, education, sample size, cognitive impairment, smoothing, and MRI field strength at $p < .0005$ and a minimum cluster size of 150 mm^3.

3.4. Local connectivity changes in Alzheimer's disease vs. mild cognitive impairment

Using voxel-wise maps coming from canonical ALE and mBF-ALE thresholded at very strong evidence analyses, no voxels of overlap were identified between the two primary data sets for both ReHo decreases and increases. Contrariwise, findings coming from the mBF-ALE thresholded at strong evidence revealed a spatial convergence of ReHo decrease in the right PCC (BA 30) and bilateral precuneus (BA 7). One cluster of convergence of ReHo increase was also identified in the left IFG (BA 44) **(Fig. S3C** and **Table S4**).

3.5. Cognitive associations

NeuroSynth association analyses uncovered quantitative associations between ReHo changes in MCI/AD and a diverse array of cognitive processes. Utilizing both canonical and mBF-ALE algorithms, we identified cognitive functions linked to peaks of ReHo variation in MCI, including learning and memory domain, such as navigation, episodic memory, memory retrieval, encoding, and spatial ability. Although both algorithms highlighted the same overall functions, a notable difference emerged in the language domain associated with the left ITG. Specifically, the mBF-ALE algorithm revealed significant associations with orthographic lexicon and phonological retrieval. Further details on the cognitive terms associated with MCI are presented in Fig. 1 and **Table S5**. In AD, ReHo alterations were characterized by the involvement of different cognitive processes within the learning and memory and social function domains, encompassing navigation, memory, autobiographical memory, social cognition, social norm processing, and mentalization (Fig. 2 and **Table S6**).

3.6. Large-Scale functional networks decomposition

The results of the functional large-scale network decomposition analysis for MCI and AD are illustrated in Figs. 1 and 2, respectively. In AD, the entire pattern of variation was associated with the default mode network (DMN), regardless of whether there was an increase or decrease in ReHo changes. In MCI, a distinct pattern emerged with the DMN prominently implicated in ReHo decreases, while the limbic network was exclusively involved in ReHo increases.

4. Discussion

To the best of our knowledge, this study offers a unique quantitative synthesis of aberrant local functional connectivity in MCI and AD compared with HCs. By employing both novel Bayesian-based and canonical versions of the ALE method, we provided evidence about the presence of consistent patterns of ReHo variation in these clinical populations, mainly localized within certain hub areas of the functionally defined default mode network. However, when stringent statistical thresholds were applied, our data-driven approach did not uncover spatial overlap of alterations between MCI and AD for both decreased and increased ReHo data. Additionally, cognitive large-scale analysis of the identified brain areas unveiled observer-independent associations with memory, language, and social functioning domains commonly impaired starting from the predementia stage of AD spectrum disease.

4.1. Altered reho in mci

The bilateral precuneus and left ITG revealed very strong evidence of local hypo-connectivity in MCI, while the right parahippocampal gyrus reported very strong evidence of local hyper-connectivity. Current findings only partially corroborate with those of the previous meta-analyses on the topic, while also introduce novel insights into the functional pathophysiology of this clinical entity. Specifically, we confirmed previous observations of ReHo decrease in the bilateral precuneus, as reported by C. Yang et al. (2023) and X. Yang et al. (2023), alongside identifying a significant ReHo increase in the right parahippocampus, a phenomenon previously highlighted solely by X. Yang et al. (2023). In contrast, our findings diverge from the early heterogeneous observations regarding ReHo alterations in several brain regions

(C. Yang et al., 2023; X. Yang et al., 2023; Zhen et al., 2018). We did not replicate, at least at very strong evidence and cluster-level FWE thresholding, patterns of increased/decreased ReHo changes in ACC, insular cortex, lingual gyrus, cerebellum, superior temporal gyrus, inferior parietal lobule, and prefrontal areas. These discrepancies may be attributed to a number of methodological factors. For example, our study leveraged the rapid expansion of the field, allowing us to integrate the largest available dataset on the topic; therefore, we optimized the balance between sensitivity and susceptibility to false positive effects, increasing the statistical power of our analysis (Eickhoff et al., 2016; Manuello et al., 2022; Müller et al., 2018). Moreover, in light of evidence from recent simulation and experimental efforts (Albajes-Eizagirre et al., 2019; Albajes-Eizagirre and Radua, 2018; Eickhoff et al., 2016), it is plausible to hypothesize that the statistical thresholding procedures and multiple comparisons correction utilized in early meta-analyses are susceptible to insufficient control over type I errors within the neuroimaging coordinate-based meta-analytic domain.

Precuneus (BA 7) has been mentioned in previous MCI research, showing gray matter atrophy (Nickl-Jockschat et al., 2012), cortical thickness reduction (Haussmann et al., 2017), accumulation of amyloid-β plaque (Mak et al., 2023), as well as reduced connectivity (Drzezga et al., 2011). Moreover, in line with our cognitive association analysis, studies have found that this area can be associated with spatial ability and egocentric navigation impairment in aMCI populations (Vlček and Laczó, 2014; Weniger et al., 2011). Independent efforts have indicated an intricate large-scale functional organization linked to the human precuneus, dividing it into anterior, central, and posterior parts (Margulies et al., 2009; Zhang and Li, 2012). Intriguingly, our decomposition analysis demonstrated that the identified cluster of local hypo-connectivity predominantly resides in the central portion of the BA 7, known for its hub role within the DMN (Cunningham et al., 2016). Therefore, this result confirms the notion that such a network is functionally impaired in MCI (Eyler et al., 2019; Joo et al., 2016) and underscores that the decreased short-range functionality of BA 7 stands out as a robust pathophysiological indication, plausibly representing effects of ongoing early neurodegeneration (Sorg et al., 2007).

We have identified voxels of ReHo decrease in the left ITG, an associative region recently found hypoperfused via arterial spin labeling in MCI patients (Thomas et al., 2021) and known to be involved in high-cognitive functions, including learning tasks and semantic language processing (Lin et al., 2020). However, it is worth noting that this finding has not been replicated in the sub-analysis focused on individuals with aMCI, even though aMCI and prodromal stages of AD are known to have a specific involvement of the inferior temporal gyrus, also with an increased synaptic loss (Scheff et al., 2011). The different sample size of the studies in MCI and aMCI as well as the clinical heterogeneity could at least partially explain this discrepancy.

Both Bayesian and canonical versions of the ALE method have revealed a statistically significant ReHo increase at the level of the right parahippocampal gyrus. This is not a surprising result, given that many studies revealed higher cortical thickness (Fernández et al., 2020), increased long-range (Penalba-Sánchez et al., 2023) and short-range (Yue et al., 2023) connectivity of this memory-related region. Previous research suggests that the ReHo increase of the BA 36 may be explained by a mechanism of compensation for the neurodegeneration of other temporo-limbic regions recruited in memory processing (Bai et al., 2008; X. Yang et al., 2023; Zhang et al., 2012) and for the functional disruption of the DMN (C. Yang et al., 2023; Zhou et al., 2014). Other authors have proposed that this phenomenon, in the context of aging and neurodegeneration, could be a temporary reorganization of regional neural activity of the connectome hub nodes due to neuroanatomical damage localized elsewhere (Damoiseaux et al., 2012; Dolcos et al., 2002; Hillary et al., 2014), followed by a structural morphometric decrease with progression of behavioral deficits (Mancuso et al., 2020; Manuello et al., 2018; Montal et al., 2018). While it is tempting to speculate about the biological meaning of the identified abnormal patterns of local connectivity, our non-invasive meta-level approach cannot directly address this issue, which remains a subject of ongoing debate (Jiang et al., 2015). In other words, the biological implications of ReHo variations in the neurological context remain unclear, emphasizing the critical need to investigate the histological and physiological basis of abnormal connectivity for distinct clinical entities.

4.2. Altered ReHo in AD

The PCC was the focus of perturbed connectivity in AD, with a concordance between mBF-ALE at very strong evidence and canonical ALE. As reported, one cluster of reduced connectivity on the right side of the PCC and one contralateral cluster of increased connectivity were evident. PCC is commonly affected in neurodegenerative diseases and particularly in AD (Zhang et al., 2024). This involvement can be seen in a more complex picture of amyloid deposition and brain atrophy spatially resembling the pattern of DMN (Buckner et al., 2005). Interestingly, PCC functional connectivity is also related to the APOE genetic status, with young healthy E4 carriers showing an increased DMN functional connectivity, as a coping strategy to overcome network inefficiency related to the at-risk APOE genotype (Filippini et al., 2009). Furthermore, considering the integrated model of PCC function (i.e., Arousal, Balance, and Breadth of Attention model; ABBA) (Leech and Sharp, 2014) a dynamic system approach can help in the understanding of the complex functioning of PCC. From this point of view, dynamic functional connectivity recently demonstrated a fine-grained fluctuation of PCC connectivity in the AD spectrum, in particular for the right PCC dynamic ReHo variability (Liao et al., 2022). Taken together, these data can partially account for the differential left/right involvement of PCC in our analysis, as a result of different pathological and compensatory mechanisms still in action in AD spectrum and potentially captured by this methodological approach.

We have observed a more circumscribed patterning of ReHo variation in AD compared to MCI. This is an unexpected result given the numerous pieces of evidence suggesting network-based damage spread in the AD course (Cauda et al., 2020; Fornari et al., 2019; Li et al., 2022; Raj and Powell, 2018). Probably, moot points are the left medial frontal gyrus, right precentral gyrus, left IFG, and bilateral temporal areas that, although found aberrant with a more liberal threshold (i.e., mBF-ALE at strong evidence), did not survive our most rigorous statistical thresholding procedures. One possible methodological explanation for this result is that the exact loci of local maximum in these brain areas differed considerably across experiments. This, and the fact that our design used x–y-z coordinates instead of three-dimensional parametric maps, could explain why no significant spatial convergences survived in this study. We also note, however, that peaks of ReHo variation in AD tend to concentrate in ventral and dorsal PCC across independent studies (Cha et al., 2015; He et al., 2007; Liao et al., 2022; Marchitelli et al., 2018; Zhang et al., 2012). In light of this, we speculate that short-range local functional connectivity aberrations may not follow the same transneural spread and connectome-based mechanisms linked to volumetric degeneration and long-range functional connectivity impairments. Future multidisciplinary research is sorely needed to disentangle this issue and to further elucidate the mechanisms underlying ReHo variations in the AD continuum.

4.3. Altered ReHo in MCI vs. AD

Patients diagnosed with MCI and AD did not exhibit voxel of alteration overlap for both decreased and increased ReHo data. This result remains consistent when conservative thresholding procedures are employed at Bayesian and FWE levels of inference, as well as when the aMCI sub-group was compared with the AD group. However, using a more liberal Bayesian force of evidence (i.e., BF $\geq$ 20) we found common clusters of local hypo-connectivity in the right PCC and bilateral precuneus. It is essential to highlight that our meta-level finding aligns

with the only two extant cross-sectional reports addressing directly this topic (Zhang et al., 2021, 2012). Interestingly, previous literature data partially support the idea of a differential involvement of precuneus and PCC in the different stages of AD pathology, with the former more involved in MCI and the latter progressively impaired in AD (Benzinger et al., 2013; Liu et al., 2008; Miners et al., 2016; Thomas et al., 2015). Beside this, we cannot also rule out a diagnostic heterogeneity in the reported clinical diagnosis across studies, as well as the inclusion of a portion of patients with an official diagnosis of AD but with a clinical picture more resembling atypical presentation of AD pathology like posterior cortical atrophy or dementia with Lewy body. Interestingly, these clinical entities are often characterized by a relative sparing of posterior cingulate/precuneus regions, defined as cingulate island sign (Whitwell et al., 2017), which can play a role in the aforementioned discrepancy among MCI and AD.

4.4. Limitations and future challenges

The current findings should be considered in light of several limitations, primarily stemming from the coordinate-based approach employed. Whether in its Bayesian or canonical form, the ALE method selectively examined local maxima of functional variation (Costa et al., 2023; Eickhoff et al., 2009), thereby overlooking other significant voxels within clusters of hypo/hyperconnectivity. While the rigorous standardization of this methodology minimizes the likelihood of spatial errors, original image-based analyses utilizing statistical parametric mapping offer superior spatial resolution and signal-to-noise ratio (Manuello et al., 2023, 2022; Müller et al., 2018). Therefore, future research endeavors could expand upon our findings by replicating them using multi-site mega-analysis designs.

Our meta-level design is also cross-sectional; thus, our short-range functional connectivity evaluation was circumscribed to a group categorization of published data about MCI/aMCI and AD. In this regard, we note that the MCI label encompasses subjects in the prodromal dementia stage but also with stable cognitive functions (Mitchell and Shiri-Feshki, 2009). While we found that patterns of variation in the aMCI subgroup largely overlapped with those of the overall MCI group, the existing literature did not allow us to fully resolve this issue due to the unavailability of biological marker analyses for detecting prodromal Alzheimer's disease in the considered cohorts. De facto, only etiological characterization utilizing biological and imaging markers, or follow-up evaluations, can reliably predict the development of Alzheimer's disease or other neurodegenerative dementias. However, follow-up studies have consistently reported a high conversion rate to AD among individuals who meet the clinical criteria for MCI. The annual conversion rate from MCI to dementia ranges from 15 % to 40 %, with those diagnosed with aMCI being at the most and closest risk of conversion (Espinosa et al., 2013; Farias et al., 2009; Geslani et al., 2005; McGrattan et al., 2022; Tabert et al., 2006; Thaipisuttikul et al., 2022). Among these individuals, approximately 80 % tend to progress to AD (Schmidtke and Hermeneit, 2008; Tábuas-Pereira et al., 2016; Visser and Verhey, 2008). Further primary research incorporating longitudinal follow-up analyses is essential to identify distinctive short-range functional connectivity profiles. Future cohorts should therefore include subjects with MCI who have undergone biological characterization and for whom ReHo data are available.

Future investigations could enhance this methodological issue by incorporating longitudinal follow-up analyses to gain deeper insights into the dynamic trajectories of ReHo aberrations in the AD continuum, particularly concerning the transition from aMCI to AD. Also, it can be argued that in analyzing the AD dataset we cannot ensure an adequate type I error control due to the limited availability of published data. While we aspire that future AD fMRI research will place greater emphasis on ReHo analyses, it is important to note that previous empirical tests have shown that the mBF-ALE algorithm effectively minimizes this type of error in such scenarios (Costa et al., 2023). Lastly, while we were able to reveal consistent and reproducible findings across the published literature, it is crucial to acknowledge the limitations of our group-level design in discerning the influence of specific critical variables (i.e., sex, level of cognitive performance or education, and sample size) that could potentially affect the replicability of functional connectivity brain research in MCI/AD (Mohtasib et al., 2022; Passamonti et al., 2019; Williamson et al., 2022; Zhu et al., 2021). We note that our post hoc meta-regression analyses did not find a significant impact of these socio-demographic and clinical variables on ReHo findings in both clinical conditions of interest. However, it is crucial to recognize that these results are derived from mean group values that may include considerable variability among subjects, especially in multicenter contexts. Therefore, these findings should be interpreted cautiously and warrant further investigation in primary ReHo research studies.

5. Conclusions

This meta-analysis provides a first quantitative synthesis about regional homogeneity aberrations in MCI and Alzheimer's disease identified over the last two-decades, providing valuable insights into a relatively underexplored area of research. Despite the heterogeneity in the literature, our meta-level approach has uncovered compelling evidence for consistent patterns of local hypo/hyperconnectivity variation in these clinical populations, predominantly localized within specific hub nodes of the human connectome. These findings represent a provisional yet insightful step toward a deeper understanding of the complex pathophysiology of these clinical entities and present promising avenues for future neuroimaging-based interventions and diagnostic MRI-based approaches.

Ethics approval and consent to participate

Not applicable.

Funding

This research was supported by the PRIN 2022 Grant (Prot. 202223XMAF; 3B4D - Blood-Based Biomarkers for Dementia: Using blood-based biomarkers to improve diagnostic discrimination between Alzheimer's disease and Frontotemporal Lobar Degeneration through Bayesian statistics) Prof. Tommaso Costa P.I.

Data and code availability statements

Data were analyzed using the minimum-Bates Factor activation likelihood estimation as implemented in the MATLAB® script available at https://figshare.com/articles/software/minimum_bayes_factor_script/17023931. Data were analyzed using the GingerALE software package (version 3.0.2) that can be freely downloaded from https://www.brainmap.org/ale/. Functional parcellations can be freely downloaded from https://surfer.nmr.mgh.harvard.edu/fswiki/CorticalParcellation_Yeo2011. Foci and functional maps are available upon reasonable request.

CRediT authorship contribution statement

Tommaso Costa: Writing – review & editing, Writing – original draft, Validation, Supervision, Software, Resources, Project administration, Methodology, Investigation, Funding acquisition, Data curation, Conceptualization. **Enrico Premi:** Writing – review & editing, Writing – original draft, Methodology. **Barbara Borroni:** Writing – review & editing, Writing – original draft, Methodology. **Jordi Manuello:** Writing – review & editing. **Franco Cauda:** Writing – review & editing. **Sergio Duca:** Writing – review & editing, Supervision. **Donato Liloia:** Writing – review & editing, Writing – original draft, Visualization, Validation,

Software, Methodology, Investigation, Formal analysis, Data curation, Conceptualization.

Declaration of competing interest

The authors report no declarations of interest.

Data availability

Data will be made available on request.

Acknowledgements

None.

Supplementary materials

Supplementary material associated with this article can be found, in the online version, at doi:10.1016/j.neuroimage.2024.120798.

References

Albajes-Eizagirre, A., Radua, J., 2018. What do results from coordinate-based meta-analyses tell us? Neuroimage 176, 550–553. https://doi.org/10.1016/j.neuroimage.2018.04.065.

Albajes-Eizagirre, A., Solanes, A., Vieta, E., Radua, J., 2019. Voxel-based meta-analysis via permutation of subject images (PSI): theory and implementation for SDM. Neuroimage 186, 174–184. https://doi.org/10.1016/j.neuroimage.2018.10.077.

Badhwar, A., Tam, A., Dansereau, C., Orban, P., Hoffstaedter, F., Bellec, P., 2017. Resting-state network dysfunction in Alzheimer's disease: a systematic review and meta-analysis. Alzheimer's Dement. 8, 73–85. https://doi.org/10.1016/j.dadm.2017.03.007.

Bai, F., Zhang, Z., Yu, H., Shi, Y., Yuan, Y., Zhu, W., Zhang, X., Qian, Y., 2008. Default-mode network activity distinguishes amnestic type mild cognitive impairment from healthy aging: a combined structural and resting-state functional MRI study. Neurosci. Lett. 438, 111–115. https://doi.org/10.1016/j.neulet.2008.04.021.

Benzinger, T.L.S., Blazey, T., Jack, C.R., Koeppe, R.A., Su, Y., Xiong, C., Raichle, M.E., Snyder, A.Z., Ances, B.M., Bateman, R.J., Cairns, N.J., Fagan, A.M., Goate, A., Marcus, D.S., Aisen, P.S., Christensen, J.J., Ercole, L., Hornbeck, R.C., Farrar, A.M., Aldea, P., Jasielec, M.S., Owen, C.J., Xie, X., Mayeux, R., Brickman, A., McDade, E., Klunk, W., Mathis, C.A., Ringman, J., Thompson, P.M., Ghetti, B., Saykin, A.J., Sperling, R.A., Johnson, K.A., Salloway, S., Correia, S., Schofield, P.R., Masters, C.L., Rowe, C., Villemagne, V.L., Martins, R., Ourselin, S., Rossor, M.N., Fox, N.C., Cash, D.M., Weiner, M.W., Holtzman, D.M., Buckles, V.D., Moulder, K., Morris, J.C., 2013. Regional variability of imaging biomarkers in autosomal dominant Alzheimer's disease. Proc. Natl. Acad. Sci. U.S.A. 110, E4502–E4509. https://doi.org/10.1073/pnas.1317918110.

Brier, M.R., Thomas, J.B., Ances, B.M., 2014. Network dysfunction in Alzheimer's disease: refining the disconnection hypothesis. Brain Connect. 4, 299. https://doi.org/10.1089/brain.2014.0236.

Buckner, R.L., Snyder, A.Z., Shannon, B.J., LaRossa, G., Sachs, R., Fotenos, A.F., Sheline, Y.I., Klunk, W.E., Mathis, C.A., Morris, J.C., Mintun, M.A., 2005. Molecular, structural, and functional characterization of Alzheimer's disease: evidence for a relationship between default activity, amyloid, and memory. J. Neurosci. 25, 7709–7717. https://doi.org/10.1523/JNEUROSCI.2177-05.2005.

Cauda, F., Mancuso, L., Nani, A., Ficco, L., Premi, E., Manuello, J., Liloia, D., Gelmini, G., Duca, S., Costa, T., 2020. Hubs of long-distance co-alteration characterize brain pathology. Hum. Brain Mapp. 41, 3878–3899. https://doi.org/10.1002/hbm.25093.

Cha, J., Hwang, J.-M., Jo, H.J., Seo, S.W., Na, D.L., Lee, J.-M., 2015. Assessment of functional characteristics of amnestic mild cognitive impairment and Alzheimer's disease using various methods of resting-state FMRI analysis. Biomed. Res. Int. 2015, 907464 https://doi.org/10.1155/2015/907464.

Costa, T., Liloia, D., Cauda, F., Fox, P.T., Mutta, F.D., Duca, S., Manuello, J., 2023. A minimum bayes factor based threshold for activation likelihood estimation. Neuroinform 21, 365–374. https://doi.org/10.1007/s12021-023-09626-6.

Costa, T., Manuello, J., Ferraro, M., Liloia, D., Nani, A., Fox, P.T., Lancaster, J., Cauda, F., 2021. BACON: a tool for reverse inference in brain activation and alteration. Hum. Brain Mapp. 42, 3343–3351. https://doi.org/10.1002/hbm.25452.

Cunningham, S.I., Tomasi, D., Volkow, N.D., 2016. Structural and functional connectivity of the precuneus and thalamus to the default mode network. Hum. Brain Mapp. 38, 938–956. https://doi.org/10.1002/hbm.23429.

Damoiseaux, J.S., Prater, K.E., Miller, B.L., Greicius, M.D., 2012. Functional connectivity tracks clinical deterioration in Alzheimer's disease. Neurobiol. Aging 33, 828. https://doi.org/10.1016/j.neurobiolaging.2011.06.024 e19–30.

Dolcos, F., Rice, H.J., Cabeza, R., 2002. Hemispheric asymmetry and aging: right hemisphere decline or asymmetry reduction. Neurosci. Biobehv. Rev. 26, 819–825. https://doi.org/10.1016/S0149-7634(02)00068-4.

Drzezga, A., Becker, J.A., Van Dijk, K.R.A., Sreenivasan, A., Talukdar, T., Sullivan, C., Schultz, A.P., Sepulcre, J., Putcha, D., Greve, D., Johnson, K.A., Sperling, R.A., 2011. Neuronal dysfunction and disconnection of cortical hubs in non-demented subjects with elevated amyloid burden. Brain 134, 1635–1646. https://doi.org/10.1093/brain/awr066.

Dubois, B., Albert, M.L., 2004. Amnestic MCI or prodromal Alzheimer's disease? Lancet Neurol. 3, 246–248. https://doi.org/10.1016/S1474-4422(04)00710-0.

Eickhoff, S.B., Bzdok, D., Laird, A.R., Kurth, F., Fox, P.T., 2012. Activation likelihood estimation meta-analysis revisited. Neuroimage 59, 2349–2361. https://doi.org/10.1016/j.neuroimage.2011.09.017.

Eickhoff, S.B., Laird, A.R., Grefkes, C., Wang, L.E., Zilles, K., Fox, P.T., 2009. Coordinate-based activation likelihood estimation meta-analysis of neuroimaging data: a random-effects approach based on empirical estimates of spatial uncertainty. Hum. Brain Mapp. 30, 2907–2926. https://doi.org/10.1002/hbm.20718.

Eickhoff, S.B., Nichols, T.E., Laird, A.R., Hoffstaedter, F., Amunts, K., Fox, P.T., Bzdok, D., Eickhoff, C.R., 2016. Behavior, sensitivity, and power of activation likelihood estimation characterized by massive empirical simulation. Neuroimage 137, 70–85. https://doi.org/10.1016/j.neuroimage.2016.04.072.

Espinosa, A., Alegret, M., Valero, S., Vinyes-Junqué, G., Hernández, I., Mauleón, A., Rosende-Roca, M., Ruiz, A., López, O., Tárraga, L., Boada, M., 2013. A longitudinal follow-up of 550 mild cognitive impairment patients: evidence for large conversion to dementia rates and detection of major risk factors involved. J. Alzheimers. Dis. 34, 769–780. https://doi.org/10.3233/JAD-122002.

Eyler, L.T., Elman, J.A., Hatton, S.N., Gough, S., Mischel, A.K., Hagler, D.J., Franz, C.E., Docherty, A., Fennema-Notestine, C., Gillespie, N., Gustavson, D., Lyons, M.J., Neale, M.C., Panizzon, M.S., Dale, A.M., Kremen, W.S., 2019. Resting state abnormalities of the default mode network in mild cognitive impairment: a systematic review and meta-analysis. J. Alzheimer's Dis. 70, 107–120. https://doi.org/10.3233/JAD-180847.

Farias, S.T., Mungas, D., Reed, B.R., Harvey, D., DeCarli, C., 2009. Progression of mild cognitive impairment to dementia in clinic- vs community-based cohorts. Arch. Neurol. 66, 1151–1157. https://doi.org/10.1001/archneurol.2009.106.

Fernández, M.Á.R., Aldrey-Vázquez, J.M., Lojo-Seoane, C., Lindín, M., Pías-Peleteiro, J. M., Vieites, A.N., Zurrón, M., Domínguez-Vivero, C., Campos-Magdaleno, M., Pereiro, A.X., Díaz, F., 2020. Cortical thickness of parahippocampal gyrus discriminates mild cognitive impairment (MCI) groups with different profiles of CSF biomarkers. Alzheimer's Dement. 16, e040944 https://doi.org/10.1002/alz.040944.

Filippini, N., MacIntosh, B.J., Hough, M.G., Goodwin, G.M., Frisoni, G.B., Smith, S.M., Matthews, P.M., Beckmann, C.F., Mackay, C.E., 2009. Distinct patterns of brain activity in young carriers of the APOE-epsilon4 allele. Proc. Natl. Acad. Sci. U.S.A. 106, 7209–7214. https://doi.org/10.1073/pnas.0811879106.

Forlenza, O.V., Diniz, B.S., Nunes, P.V., Memória, C.M., Yassuda, M.S., Gattaz, W.F., 2009. Diagnostic transitions in mild cognitive impairment subtypes. Int. Psychogeriatr. 21, 1088–1095. https://doi.org/10.1017/S1041610209990792.

Fornari, S., Schäfer, A., Jucker, M., Goriely, A., Kuhl, E., 2019. Prion-like spreading of Alzheimer's disease within the brain's connectome. J. R. Soc. Interface 16, 20190356. https://doi.org/10.1098/rsif.2019.0356.

Geslani, D.M., Tierney, M.C., Herrmann, N., Szalai, J.P., 2005. Mild cognitive impairment: an operational definition and its conversion rate to Alzheimer's disease. Dement. Geriatr. Cogn. Disord. 19, 383–389. https://doi.org/10.1159/000084709.

Hansen, J.Y., Markello, R.D., Vogel, J.W., Seidlitz, J., Bzdok, D., Misic, B., 2021. Mapping gene transcription and neurocognition across human neocortex. Nat. Hum. Behav. 5, 1240–1250. https://doi.org/10.1038/s41562-021-01082-z.

Haussmann, R., Werner, A., Gruschwitz, A., Osterrath, A., Lange, J., Donix, K.L., Linn, J., Donix, M., 2017. Precuneus structure changes in amnestic mild cognitive impairment. Am. J. Alzheimers. Dis. Other Demen. 32, 22–26. https://doi.org/10.1177/1533317516678087.

He, Y., Wang, L., Zang, Y., Tian, L., Zhang, X., Li, K., Jiang, T., 2007. Regional coherence changes in the early stages of Alzheimer's disease: a combined structural and resting-state functional MRI study. Neuroimage 35, 488–500. https://doi.org/10.1016/j.neuroimage.2006.11.042.

Hillary, F.G., Rajtmajer, S.M., Roman, C.A., Medaglia, J.D., Slocomb-Dluzen, J.E., Calhoun, V.D., Good, D.C., Wylie, G.R., 2014. The rich get richer: brain injury elicits hyperconnectivity in core subnetworks. PLoS ONE 9, e104021. https://doi.org/10.1371/journal.pone.0104021.

Ibrahim, B., Suppiah, S., Ibrahim, N., Mohamad, M., Hassan, H.A., Nasser, N.S., Saripan, M.I., 2021. Diagnostic power of resting-state fMRI for detection of network connectivity in Alzheimer's disease and mild cognitive impairment: a systematic review. Hum. Brain Mapp. 42, 2941. https://doi.org/10.1002/hbm.25369.

Jiang, L., Xu, T., He, Ye, Hou, X.-H., Wang, J., Cao, X.-Y., Wei, G.-X., Yang, Z., He, Yong, Zuo, X.-N., 2015. Toward neurobiological characterization of functional homogeneity in the human cortex: regional variation, morphological association and functional covariance network organization. Brain Struct. Funct. 220, 2485–2507. https://doi.org/10.1007/s00429-014-0795-8.

Jiang, L., Zuo, X.-N., 2016. Regional homogeneity: a multimodal, multiscale neuroimaging marker of the human connectome. Neuroscientist. 22, 486–505. https://doi.org/10.1177/1073858415595004.

Joo, S.H., Lim, H.K., Lee, C.U., 2016. Three large-scale functional brain networks from resting-state functional MRI in subjects with different levels of cognitive impairment. Psychiatry Investig. 13, 1–7. https://doi.org/10.4306/pi.2016.13.1.1.

Kass, R.E., Raftery, A.E., 1995. Bayes factors. J. Am. Stat. Assoc. 90, 773–795. https://doi.org/10.2307/2291091.

Klekociuk, S.Z., Saunders, N.L., Summers, M.J., 2016. Diagnosing mild cognitive impairment as a precursor to dementia: fact or fallacy? Aust. Psychol. 51, 366–373. https://doi.org/10.1111/ap.12178.

Laird, A.R., Robinson, J.L., McMillan, K.M., Tordesillas-Gutiérrez, D., Moran, S.T., Gonzales, S.M., Ray, K.L., Franklin, C., Glahn, D.C., Fox, P.T., Lancaster, J.L., 2010. Comparison of the disparity between Talairach and MNI coordinates in functional neuroimaging data: validation of the Lancaster transform. Neuroimage 51, 677–683. https://doi.org/10.1016/j.neuroimage.2010.02.048.

Leech, R., Sharp, D.J., 2014. The role of the posterior cingulate cortex in cognition and disease. Brain 137, 12–32. https://doi.org/10.1093/brain/awt162.

Li, W., Yang, D., Yan, C., Chen, M., Li, Q., Zhu, W., Wu, G., 2022. Characterizing network selectiveness to the dynamic spreading of neuropathological events in Alzheimer's disease. J. Alzheimers. Dis. 86, 1805–1816. https://doi.org/10.3233/JAD-215596.

Liao, Z., Sun, W., Liu, X., Guo, Z., Mao, D., Yu, E., Chen, Y., 2022. Altered dynamic intrinsic brain activity of the default mode network in Alzheimer's disease: a resting-state fMRI study. Front. Hum. Neurosci. 16, 951114 https://doi.org/10.3389/fnhum.2022.951114.

Liloia, D., Cauda, F., Uddin, L.Q., Manuello, J., Mancuso, L., Keller, R., Nani, A., Costa, T., 2023. Revealing the selectivity of neuroanatomical alteration in autism spectrum disorder via reverse inference. Biol. Psychiatry Cognit. Neurosci. Neuroimaging 8, 1075–1083. https://doi.org/10.1016/j.bpsc.2022.01.007.

Liloia, D., Mancuso, L., Uddin, L.Q., Costa, T., Nani, A., Keller, R., Manuello, J., Duca, S., Cauda, F., 2021. Gray matter abnormalities follow non-random patterns of co-alteration in autism: meta-connectomic evidence. NeuroImage Clinical 30, 102583. https://doi.org/10.1016/j.nicl.2021.102583.

Liloia, D., Manuello, J., Costa, T., Keller, R., Nani, A., Cauda, F., 2024a. Atypical local brain connectivity in pediatric autism spectrum disorder? A coordinate-based meta-analysis of regional homogeneity studies. Eur. Arch. Psychiatry Clin. Neurosci. 274, 3–18. https://doi.org/10.1007/s00406-022-01541-2.

Liloia, D., Zamfira, D.A., Tanaka, M., Manuello, J., Crocetta, A., Keller, R., Cozzolino, M., Duca, S., Cauda, F., Costa, T., 2024b. Disentangling the role of gray matter volume and concentration in autism spectrum disorder: a meta-analytic investigation of 25 years of voxel-based morphometry research. Neurosci. Biobehv. Rev. 164, 105791 https://doi.org/10.1016/j.neubiorev.2024.105791.

Lin, Y.-H., Young, I.M., Conner, A.K., Glenn, C.A., Chakraborty, A.R., Nix, C.E., Bai, M.Y., Dhanaraj, V., Fonseka, R.D., Hormovas, J., Tanglay, O., Briggs, R.G., Sughrue, M.E., 2020. Anatomy and white matter connections of the inferior temporal gyrus. World Neurosurg. 143, e656–e666. https://doi.org/10.1016/j.wneu.2020.08.058.

Liu, L., Jiang, H., Wang, D., Zhao, X., 2021. A study of regional homogeneity of resting-state functional magnetic resonance imaging in mild cognitive impairment. Behav. Brain Res. 402, 113103 https://doi.org/10.1016/j.bbr.2020.113103.

Liu, Y., Wang, K., Yu, C., He, Y., Zhou, Y., Liang, M., Wang, L., Jiang, T., 2008. Regional homogeneity, functional connectivity and imaging markers of Alzheimer's disease: a review of resting-state fMRI studies. Neuropsychologia 46, 1648–1656. https://doi.org/10.1016/j.neuropsychologia.2008.01.027.

Mak, E., Zhang, L., Tan, C.H., Reilhac, A., Shim, H.Y., Wen, M.O.Q., Wong, Z.X., Chong, E.J.Y., Xu, X., Stephenson, M., Venketasubramanian, N., Zhou, J.H., O'Brien, J.T., Chen, C.L.-H., 2023. Longitudinal associations between β-amyloid and cortical thickness in mild cognitive impairment. Brain Commun. 5, fcad192. https://doi.org/10.1093/braincomms/fcad192.

Mancuso, L., Fornito, A., Costa, T., Ficco, L., Liloia, D., Manuello, J., Duca, S., Cauda, F., 2020. A meta-analytic approach to mapping co-occurrent grey matter volume increases and decreases in psychiatric disorders. Neuroimage 222, 117220. https://doi.org/10.1016/j.neuroimage.2020.117220.

Manuello, J., Costa, T., Cauda, F., Liloia, D., 2022. Six actions to improve detection of critical features for neuroimaging coordinate-based meta-analysis preparation. Neurosci. Biobehv. Rev. 137, 104659 https://doi.org/10.1016/j.neubiorev.2022.104659.

Manuello, J., Liloia, D., Crocetta, A., Cauda, F., Costa, T., 2023. CBMAT: a MATLAB toolbox for data preparation and post hoc analyses in neuroimaging meta-analyses. Behav. Res. https://doi.org/10.3758/s13428-023-02185-3.

Manuello, J., Nani, A., Premi, E., Borroni, B., Costa, T., Tatu, K., Liloia, D., Duca, S., Cauda, F., 2018. The pathoconnectivity profile of Alzheimer's disease: a morphometric coalteration network analysis. Front. Neurol. 8 https://doi.org/10.3389/fneur.2017.00739.

Marchitelli, R., Aiello, M., Cachia, A., Quarantelli, M., Cavaliere, C., Postiglione, A., Tedeschi, G., Montella, P., Milan, G., Salvatore, M., Salvatore, E., Baron, J.C., Pappatà, S., 2018. Simultaneous resting-state FDG-PET/fMRI in Alzheimer disease: relationship between glucose metabolism and intrinsic activity. Neuroimage 176, 246–258. https://doi.org/10.1016/j.neuroimage.2018.04.048.

Margulies, D.S., Vincent, J.L., Kelly, C., Lohmann, G., Uddin, L.Q., Biswal, B.B., Villringer, A., Castellanos, F.X., Milham, M.P., Petrides, M., 2009. Precuneus shares intrinsic functional architecture in humans and monkeys. Proc. Natl. Acad. Sci. U.S.A. 106, 20069–20074. https://doi.org/10.1073/pnas.0905314106.

Márquez, F., Yassa, M.A., 2019. Neuroimaging biomarkers for Alzheimer's disease. Mol. Neurodegener. 14, 21. https://doi.org/10.1186/s13024-019-0325-5.

McGrattan, A.M., Pakpahan, E., Siervo, M., Mohan, D., Reidpath, D.D., Prina, M., Allotey, P., Zhu, Y., Shulin, C., Yates, J., Paddick, S.-M., Robinson, L., Stephan, B.C. M., DePEC team, 2022. Risk of conversion from mild cognitive impairment to dementia in low- and middle-income countries: a systematic review and meta-analysis. Alzheimers Dement (N Y) 8, e12267. https://doi.org/10.1002/trc2.12267.

Min, J., Zhou, X.-X., Zhou, F., Tan, Y., Wang, W.-D., 2019. A study on changes of the resting-state brain function network in patients with amnestic mild cognitive impairment. Braz. J. Med. Biol. Res. 52, e8244. https://doi.org/10.1590/1414-431X20198244.

Miners, J.S., Palmer, J.C., Love, S., 2016. Pathophysiology of hypoperfusion of the Precuneus in early Alzheimer's disease. Brain Pathol. 26, 533–541. https://doi.org/10.1111/bpa.12331.

Mitchell, A.J., Shiri-Feshki, M., 2009. Rate of progression of mild cognitive impairment to dementia–meta-analysis of 41 robust inception cohort studies. Acta Psychiatr. Scand. 119, 252–265. https://doi.org/10.1111/j.1600-0447.2008.01326.x.

Mohtasib, R., Alghamdi, J., Jobeir, A., Masawi, A., Pedrosa de Barros, N., Billiet, T., Struyfs, H., Phan, T.V., Van Hecke, W., Ribbens, A., 2022. MRI biomarkers for Alzheimer's disease: the impact of functional connectivity in the default mode network and structural connectivity between lobes on diagnostic accuracy. Heliyon 8, e08901. https://doi.org/10.1016/j.heliyon.2022.e08901.

Montal, V., Vilaplana, E., Alcolea, D., Pegueroles, J., Pasternak, O., González-Ortiz, S., Clarimón, J., Carmona-Iragui, M., Illán-Gala, I., Morenas-Rodríguez, E., Ribosa-Nogué, R., Sala, I., Sánchez-Saudinós, M.-B., García-Sebastian, M., Villanúa, J., Izagirre, A., Estanga, A., Ecay-Torres, M., Iriondo, A., Clerigue, M., Tainta, M., Pozueta, A., González, A., Martínez-Heras, E., Llufriu, S., Blesa, R., Sanchez-Juan, P., Martínez-Lage, P., Lleó, A., Fortea, J., 2018. Cortical microstructural changes along the Alzheimer's disease continuum. Alzheimers Dement 14, 340–351. https://doi.org/10.1016/j.jalz.2017.09.013.

Müller, V.I., Cieslik, E.C., Laird, A.R., Fox, P.T., Radua, J., Mataix-Cols, D., Tench, C.R., Yarkoni, T., Nichols, T.E., Turkeltaub, P.E., Wager, T.D., Eickhoff, S.B., 2018. Ten simple rules for neuroimaging meta-analysis. Neurosci. Biobehav. Rev. 84, 151–161. https://doi.org/10.1016/j.neubiorev.2017.11.012.

Nickl-Jockschat, T., Kleiman, A., Schulz, J.B., Schneider, F., Laird, A.R., Fox, P.T., Eickhoff, S.B., Reetz, K., 2012. Neuroanatomic changes and their association with cognitive decline in mild cognitive impairment: a meta-analysis. Brain Struct. Funct. 217, 115–125. https://doi.org/10.1007/s00429-011-0333-x.

Page, M.J., McKenzie, J.E., Bossuyt, P.M., Boutron, I., Hoffmann, T.C., Mulrow, C.D., Shamseer, L., Tetzlaff, J.M., Akl, E.A., Brennan, S.E., Chou, R., Glanville, J., Grimshaw, J.M., Hróbjartsson, A., Lalu, M.M., Li, T., Loder, E.W., Mayo-Wilson, E., McDonald, S., McGuinness, L.A., Stewart, L.A., Thomas, J., Tricco, A.C., Welch, V.A., Whiting, P., Moher, D., 2021. The PRISMA 2020 statement: an updated guideline for reporting systematic reviews. PLoS. Med. 18, e1003583 https://doi.org/10.1371/journal.pmed.1003583.

Passamonti, L., Tsvetanov, K.A., Jones, P.S., Bevan-Jones, W.R., Arnold, R., Borchert, R. J., Mak, E., Su, L., O'Brien, J.T., Rowe, J.B., 2019. Neuroinflammation and functional connectivity in Alzheimer's disease: interactive influences on cognitive performance. J. Neurosci. 39, 7218–7226. https://doi.org/10.1523/JNEUROSCI.2574-18.2019.

Penalba-Sánchez, L., Oliveira-Silva, P., Sumich, A.L., Cifre, I., 2023. Increased functional connectivity patterns in mild Alzheimer's disease: a rsfMRI study. Front. Aging Neurosci. 14, 1037347 https://doi.org/10.3389/fnagi.2022.1037347.

Peraza, L.R., Colloby, S.J., Deboys, L., O'Brien, J.T., Kaiser, M., Taylor, J.-P., 2016. Regional functional synchronizations in dementia with Lewy bodies and Alzheimer's disease. Int. Psychogeriatr. 28, 1143–1151. https://doi.org/10.1017/S1041610216000429.

Petersen, R.C., Caracciolo, B., Brayne, C., Gauthier, S., Jelic, V., Fratiglioni, L., 2014. Mild cognitive impairment: a concept in evolution. J. Intern. Med. 275, 214–228. https://doi.org/10.1111/joim.12190.

Poldrack, R., Kittur, A., Kalar, D., Miller, E., Seppa, C., Gil, Y., Parker, D., Sabb, F., Bilder, R., 2011. The cognitive atlas: toward a knowledge foundation for cognitive neuroscience. Front. Neuroinform. 5.

Radua, J., Mataix-Cols, D., Phillips, M.L., El-Hage, W., Kronhaus, D.M., Cardoner, N., Surguladze, S., 2012. A new meta-analytic method for neuroimaging studies that combines reported peak coordinates and statistical parametric maps. Eur. Psychiatry 27, 605–611. https://doi.org/10.1016/j.eurpsy.2011.04.001.

Raj, A., Powell, F., 2018. Models of network spread and network degeneration in brain disorders. Biol. Psychiatry Cognit. Neurosci. Neuroimaging 3, 788–797. https://doi.org/10.1016/j.bpsc.2018.07.012.

Scheff, S.W., Price, D.A., Schmitt, F.A., Scheff, M.A., Mufson, E.J., 2011. Synaptic loss in the inferior temporal gyrus in mild cognitive impairment and Alzheimer's disease. J. Alzheimers. Dis. 24, 547–557. https://doi.org/10.3233/JAD-2011-101782.

Schmidtke, K., Hermeneit, S., 2008. High rate of conversion to Alzheimer's disease in a cohort of amnestic MCI patients. Int. Psychogeriatr. 20, 96–108. https://doi.org/10.1017/S1041610207005509.

Sorg, C., Riedl, V., Mühlau, M., Calhoun, V.D., Eichele, T., Läer, L., Drzezga, A., Förstl, H., Kurz, A., Zimmer, C., Wohlschläger, A.M., 2007. Selective changes of resting-state networks in individuals at risk for Alzheimer's disease. Proc. Natl. Acad. Sci. U.S.A. 104, 18760–18765. https://doi.org/10.1073/pnas.0708803104.

Tabert, M.H., Manly, J.J., Liu, X., Pelton, G.H., Rosenblum, S., Jacobs, M., Zamora, D., Goodkind, M., Bell, K., Stern, Y., Devanand, D.P., 2006. Neuropsychological prediction of conversion to Alzheimer disease in patients with mild cognitive impairment. Arch. Gen. Psychiatry 63, 916–924. https://doi.org/10.1001/archpsyc.63.8.916.

Tábuas-Pereira, M., Baldeiras, I., Duro, D., Santiago, B., Ribeiro, M.H., Leitão, M.J., Oliveira, C., Santana, I., 2016. Prognosis of early-onset vs. late-onset mild cognitive impairment: comparison of conversion rates and its predictors. Geriatrics (Basel) 1, 11. https://doi.org/10.3390/geriatrics1020011.

Thaipisuttikul, P., Jaikla, K., Satthong, S., Wisajun, P., 2022. Rate of conversion from mild cognitive impairment to dementia in a Thai hospital-based population: a retrospective cohort. Alzheimers Dement (N Y) 8, e12272. https://doi.org/10.1002/trc2.12272.

Thomas, K.R., Osuna, J.R., Weigand, A.J., Edmonds, E.C., Clark, A.L., Holmqvist, S., Cota, I.H., Wierenga, C.E., Bondi, M.W., Bangen, K.J., Alzheimer's Disease Neuroimaging Initiative, 2021. Regional hyperperfusion in older adults with objectively-defined subtle cognitive decline. J. Cereb. Blood Flow Metab. 41, 1001–1012. https://doi.org/10.1177/0271678X20935171.

Thomas, T., Miners, S., Love, S., 2015. Post-mortem assessment of hypoperfusion of cerebral cortex in Alzheimer's disease and vascular dementia. Brain 138, 1059–1069. https://doi.org/10.1093/brain/awv025.

Visser, P.J., Verhey, F.R.J., 2008. Mild cognitive impairment as predictor for Alzheimer's disease in clinical practice: effect of age and diagnostic criteria. Psychol. Med. 38, 113–122. https://doi.org/10.1017/S0033291707000554.

Vlček, K., Laczó, J., 2014. Neural correlates of spatial navigation changes in mild cognitive impairment and Alzheimer's disease. Front. Behav. Neurosci. 8 https://doi.org/10.3389/fnbeh.2014.00089.

Wang, S.-M., Kim, N.-Y., Kang, D.W., Um, Y.H., Na, H.-R., Woo, Y.S., Lee, C.U., Bahk, W.-M., Lim, H.K., 2021. A comparative study on the predictive value of different resting-state functional magnetic resonance imaging parameters in preclinical Alzheimer's disease. Front. Psychiatry 12, 626332. https://doi.org/10.3389/fpsyt.2021.626332.

Weniger, G., Ruhleder, M., Lange, C., Wolf, S., Irle, E., 2011. Egocentric and allocentric memory as assessed by virtual reality in individuals with amnestic mild cognitive impairment. Neuropsychologia 49, 518–527. https://doi.org/10.1016/j.neuropsychologia.2010.12.031.

Whitwell, J.L., Graff-Radford, J., Singh, T.D., Drubach, D.A., Senjem, M.L., Spychalla, A. J., Tosakulwong, N., Lowe, V.J., Josephs, K.A., 2017. 18F-FDG PET in posterior cortical atrophy and dementia with Lewy bodies. J. Nucl. Med. 58, 632–638. https://doi.org/10.2967/jnumed.116.179903.

Williamson, J., Yabluchanskiy, A., Mukli, P., Wu, D.H., Sonntag, W., Ciro, C., Yang, Y., 2022. Sex differences in brain functional connectivity of hippocampus in mild cognitive impairment. Front. Aging Neurosci. 14, 959394 https://doi.org/10.3389/fnagi.2022.959394.

Yang, C., Gao, X., Liu, N., Sun, H., Gong, Q., Yao, L., Lui, S., 2023a. Convergent and distinct neural structural and functional patterns of mild cognitive impairment: a multimodal meta-analysis. Cereb. Cortex. 33, 8876–8889. https://doi.org/10.1093/cercor/bhad167.

Yang, X., Wu, H., Song, Y., Chen, S., Ge, H., Yan, Z., Yuan, Q., Liang, X., Lin, X., Chen, J., 2023b. Functional MRI-specific alterations in frontoparietal network in mild cognitive impairment: an ALE meta-analysis. Front. Aging Neurosci. 15, 1165908 https://doi.org/10.3389/fnagi.2023.1165908.

Yarkoni, T., Poldrack, R.A., Nichols, T.E., Van Essen, D.C., Wager, T.D., 2011. Large-scale automated synthesis of human functional neuroimaging data. Nat. Methods 8, 665–670. https://doi.org/10.1038/nmeth.1635.

Yeo, B.T.T., Krienen, F.M., Sepulcre, J., Sabuncu, M.R., Lashkari, D., Hollinshead, M., Roffman, J.L., Smoller, J.W., Zöllei, L., Polimeni, J.R., Fischl, B., Liu, H., Buckner, R. L., 2011. The organization of the human cerebral cortex estimated by intrinsic functional connectivity. J. Neurophysiol. 106, 1125–1165. https://doi.org/10.1152/jn.00338.2011.

Yuan, X., Han, Y., Wei, Y., Xia, M., Sheng, C., Jia, J., He, Y., 2016. Regional homogeneity changes in amnestic mild cognitive impairment patients. Neurosci. Lett. 629, 1–8. https://doi.org/10.1016/j.neulet.2016.06.047.

Yue, J., Han, S.-W., Liu, X., Wang, S., Zhao, W.-W., Cai, L.-N., Cao, D.-N., Mah, J.Z., Hou, Y., Cui, X., Wang, Y., Chen, L., Li, A., Li, X.-L., Yang, G., Zhang, Q., 2023. Functional brain activity in patients with amnestic mild cognitive impairment: an rs-fMRI study. Front. Neurol. 14, 1244696 https://doi.org/10.3389/fneur.2023.1244696.

Zang, Y., Jiang, T., Lu, Y., He, Y., Tian, L., 2004. Regional homogeneity approach to fMRI data analysis. Neuroimage 22, 394–400. https://doi.org/10.1016/j.neuroimage.2003.12.030.

Zhang, Q., Fan, C., Wang, L., Li, T., Wang, M., Han, Y., Jiang, J., Alzheimer's Disease Neuroimaging Initiative, 2024. Glucose metabolism in posterior cingulate cortex has supplementary value to predict the progression of cognitively unimpaired to dementia due to Alzheimer's disease: an exploratory study of 18F-FDG-PET. Geroscience 46, 1407–1420. https://doi.org/10.1007/s11357-023-00897-0.

Zhang, Q., Wang, Q., He, C., Fan, D., Zhu, Y., Zang, F., Tan, C., Zhang, S., Shu, H., Zhang, Z., Feng, H., Wang, Z., Xie, C., 2021. Altered regional cerebral blood flow and brain function across the Alzheimer's disease spectrum: a potential biomarker. Front. Aging Neurosci. 13, 630382 https://doi.org/10.3389/fnagi.2021.630382.

Zhang, S., Li, C.R., 2012. Functional connectivity mapping of the human precuneus by resting state fMRI. Neuroimage 59, 3548. https://doi.org/10.1016/j.neuroimage.2011.11.023.

Zhang, Z., Liu, Y., Jiang, T., Zhou, B., An, N., Dai, H., Wang, P., Niu, Y., Wang, L., Zhang, X., 2012. Altered spontaneous activity in Alzheimer's disease and mild cognitive impairment revealed by Regional Homogeneity. Neuroimage 59, 1429–1440. https://doi.org/10.1016/j.neuroimage.2011.08.049.

Zhen, D., Xia, W., Yi, Z.Q., Zhao, P.W., Zhong, J.G., Shi, H.C., Li, H.L., Dai, Z.Y., Pan, P.L., 2018. Alterations of brain local functional connectivity in amnestic mild cognitive impairment. Transl. Neurodegener. 7, 26. https://doi.org/10.1186/s40035-018-0134-8.

Zhou, X., Zhang, J., Chen, Y., Ma, T., Wang, Y., Wang, J., Zhang, Z., 2014. Aggravated cognitive and brain functional impairment in mild cognitive impairment patients with type 2 diabetes: a resting-state functional MRI study. J. Alzheimers. Dis. 41, 925–935. https://doi.org/10.3233/JAD-132354.

Zhu, W., Li, Xiaoshu, Li, Xiaohu, Wang, H., Li, M., Gao, Z., Wu, X., Tian, Y., Zhou, S., Wang, K., Yu, Y., 2021. The protective impact of education on brain structure and function in Alzheimer's disease. BMC. Neurol. 21, 423. https://doi.org/10.1186/s12883-021-02445-9.

Zuo, X.-N., Xu, T., Jiang, L., Yang, Z., Cao, X.-Y., He, Y., Zang, Y.-F., Castellanos, F.X., Milham, M.P., 2013. Toward reliable characterization of functional homogeneity in the human brain: preprocessing, scan duration, imaging resolution and computational space. Neuroimage 65, 374–386. https://doi.org/10.1016/j.neuroimage.2012.10.017.